Original Article

Flow characteristics of positive and negative pressure irrigation in an immature tooth – A computational fluid dynamics study

Selventhra Savitha, Nitin Kumar[1], Vamsi Krishna Chalamalla[1], Sidhartha Sharma, Vijay Kumar, Amrita Chawla, Ajay Logani

Division of Conservative Dentistry and Endodontics, Centre for Dental Education and Research, All India Institute of Medical Sciences, [1]Department of Applied Mechanics, Indian Institute of Technology, New Delhi, India

Abstract

Aim: This study aims to investigate the irrigation dynamics in an immature tooth during positive and negative pressure irrigation using a computational fluid dynamics (CFDs) model.

Materials and Methods: Cone-beam computed tomography scan of the maxillary central incisor with Cvek's stage III root development was used for the reconstruction of the root canal geometry. The computer-aided design models of open (front vent and notched) and closed (side vent [SV]) needles were positioned inside the root canal at two penetration depths, i.e., 3 mm and 1 mm short of apex. The negative pressure microcannula (MiC) was positioned at the level of the root apex. A prevalidated CFD model was used to simulate endodontic irrigation.

Results: The irrigant velocity in the apical root canal beyond the needle tip exceeded 0.1 m/s. As the needles were positioned closer to the apex, the wall shear stress (WSS) increased for the open-ended needles and decreased for the SV needle. MiC produced the lowest WSS. The mean apical pressure produced by the SV needle and MiC were below the critical threshold for periapical extrusion.

Conclusions: The SV needle inserted within 1–3 mm of root apex during endodontic irrigation in an immature tooth allows adequate irrigant exchange with minimal risk of periapical extrusion.

Keywords: Computational fluid dynamics; endodontic irrigation; immature teeth; open apex

INTRODUCTION

The optimal disinfection of the root canal space by chemomechanical preparation is the foundation for a favorable endodontic outcome.[1] Irrigation is the mainstay for disinfection protocol for immature roots with thin dentinal walls where minimal or no instrumentation is recommended.[2]

Address for correspondence:
Dr. Vijay Kumar,
Room No. 308, 3rd Floor, Division of Conservative Dentistry and Endodontics, Centre for Dental Education and Research, All India Institute of Medical Sciences, New Delhi - 110 029, India.
E-mail: kumarvijay29@gmail.com

Date of submission : 14.04.2023
Review completed : 07.06.2023
Date of acceptance : 05.07.2023
Published : 16.09.2023

Access this article online	
Quick Response Code:	Website: https://journals.lww.com/jcde
	DOI: 10.4103/jcd.jcd_240_23

The method of mathematically simulating a physical phenomenon involving fluid flow and solving it numerically using a computational procedure is known as computational fluid dynamics (CFDs). It has been used in endodontics to investigate the effect of root canal anatomy, needle diameter, penetration depth, tip design and bevel orientation, irrigant delivery velocity, and pressure on irrigation dynamics and root canal disinfection.[3,4]

Previous CFD investigations on endodontic irrigation were conducted in the tapered root canal with a limited apical opening simulating a mature permanent tooth.[5] However,

How to cite this article: Savitha S, Kumar N, Chalamalla VK, Sharma S, Kumar V, Chawla A, *et al*. Flow characteristics of positive and negative pressure irrigation in an immature tooth – A computational fluid dynamics study. J Conserv Dent Endod 2023;26:544-9.

the findings of these studies cannot be applied to a tooth with an immature root, which, in contrast, has divergent walls and a wide-open apex. Limited *in vitro* studies have quantified the apical pressure, and volume of irrigant extruded during irrigation in teeth with immature apices using different irrigation delivery systems.[6-8] No data on the fluid dynamics of endodontic irrigation in immature teeth are available. Therefore, the present study was designed to evaluate the effect of positive and negative pressure irrigant delivery systems on fluid dynamics during endodontic irrigation in teeth with immature apex using the prevalidated CFD model.

MATERIALS AND METHODS

The Ethical Clearance was obtained from the Institute Research Ethics Committee (Ref. No. IECPG-231/24.06.2020). The study was conducted according to the principles of Helsinki and written informed consent was obtained from participants. The objectives of the study were to analyze the irrigation dynamics parameters, i.e., velocity, flow pattern, shear stress, and apical pressure in immature maxillary central incisor. In addition, the parameters of irrigation efficiency, i.e., clean depth (irrigant touching the root canal wall along the vertical axis) and clean span (irrigant touching the root canal wall along the cross axis)[9] were evaluated.

A cone beam computed tomography (CBCT) scan (3 × 3 FOV; 0.125 µm voxel size) of permanent maxillary central incisor tooth with Cvek's stage III root development without any resorptive/developmental defect or root canal filling was identified from the Institutional database. The root canal geometry up to the cementoenamel junction was segmented and reconstructed in Step. Format using Mimics® (Materialise, Leuven, Belgium).

Previously described dimensions[10] were used to reconstruct irrigation needle designs using computer-aided design (CAD) software (SolidWorks 2016 × 64 Edition, Dassault Systems, Paris, France). The positive pressure needles (30-gauge, Internal diameter = 190 µm, External diameter = 300 µm) had two open-ended (front vent [FV] and Notched) and one closed-ended (side vent [SV]) tip design. The endodontic microcannula (MiC) (28-Gauge) was used for negative pressure irrigation. It featured a closed spherical end and twelve evacuation holes in four rows of three, each measuring 0.1 mm in diameter. The length of all the needles used was set to 31 mm to ensure uniformity [Table 1].

The reconstructed three-dimensional (3D) root canal geometry was uploaded in Solid Works CAD software. The root canal model measured 10.5 mm in length. The CAD-designed positive pressure needles were positioned in the root canal model as centered as possible at 3 mm and 1 mm from the root apex. Micro-cannula was positioned at the root apex. This resulted in a total of seven geometries of fluid domain with positive and negative pressure needles in the root canal model.

Table 1: Type of needle, tip design, and insertion depths used in the present study

Type of irrigation	Type of needle	Tip design	Needle insertion depth from apex (mm)	
Positive pressure	Open-ended	Front vent	3	1
		Notched	3	1
	Closed-ended	Side vent	3	1
Negative pressure	Closed-ended	MiC	At apex	

MiC: Microcannula

The fluid domain geometries were imported into ANSYS 19.2 FLUENT (Fluent Inc., Lebanon, NH, USA). The fluid was considered to be filled inside the needle and the root canal model. The inlet, outlet, and walls of the fluid domain were defined. A hybrid mesh of 1 million (1–1.1 million) quadratic tetrahedral elements was created and refined at the needle and the root canal walls. The mesh quality was checked to make sure it was within normal limits for skewness and orthogonality. The grid Independence study was conducted; a transient flow simulation was performed. The walls of the root canal and the irrigation elements were assumed to be rigid and impermeable, and no-slip boundary conditions were applied. The gravitational constant was set to 9.8 m/s^2 along the long axis of the root canal model. In the positive pressure irrigation simulation, the axial inlet velocity of 8.6 m/s consistent with the flow rate of 0.26 ml/s was applied at the needle inlet.[11] The root canal outlet was subjected to atmospheric pressure. In the negative pressure irrigation simulation, an aspiration pressure of 97.5 mmHg was applied at the needle outlet, and the atmospheric pressure was applied at the root canal inlet.[10] The irrigant was modeled as incompressible, Newtonian, homogeneous, and isothermal fluid with characteristics similar to the 2.5% sodium hypochlorite (NaOCl, density = 1060 kg/m^3, viscosity = 1.073×10^{-3} kgm^{-1} s^{-1}).[12] The Shear Stress Transport-K omega (SST-K omega) turbulence model was employed to model the Reynolds stresses. The backflow turbulent intensity and the viscosity ratio were set up at 5% and 10. Every transport equation was discretized to have the accuracy of at least second order. With a time step size of 10-4 s, the convergence threshold was set to 10-5 of the highest scaled residuals.

RESULTS

Flow pattern

The irrigant jet streams were oriented toward the root apex in open-ended needles and toward the canal wall at an angle of 60° to the long axis of the SV needle at the needle exit. The irrigant from the canal orifice flowed toward the apex in the case of negative pressure irrigation simulations. The irrigant flow pattern was unaffected by the needle penetration depth. All the simulations revealed irrigant replenishment in the apical region of the root canal [Figure 1a].

Irrigant velocity

For appropriate irrigant replacement, the effective velocity above 0.1 m/s was deemed clinically relevant.[11] The maximum irrigant velocity (12.4 m/s) was achieved inside the needle lumen in all positive-pressure needles. There was a decrease in the irrigant velocity as the irrigant exited the needle outlet. The irrigant axial velocity was ≥1 m/s for both open-ended needles irrespective of the needle penetration depth. For the SV needle, as the irrigant approached the apex, the irrigant axial velocity decreased to <1 m/s. The maximum irrigant velocity achieved was 2.3 m/s inside the lumen of MiC [Figure 1b].

Wall shear stress

The critical shear stress of 100 Pa was considered for effective biofilm and smear layer removal.[9] Wall shear stress (WSS) increased for open-ended needles and reduced for SV needles as the needle tip moved closer to the apex. SV needle generated the highest WSS when positioned 3 mm from the apex, followed by FV and notched needles. However, the FV needle produced the highest WSS, followed by notched and SV needles, at a needle penetration depth of 1 mm from the apex. The WSS was evenly distributed in the apical portion above the tip of FV needle. WSS was concentrated on the wall facing away and towards the vent for notched and SV needles, respectively. The least WSS were generated by MiC which was evenly distributed throughout the canal wall [Figure 2a].

Mean apical pressure

The maximum mean apical pressure (MAP) was produced by FV needles followed by notched and SV needles. Irrespective of needle penetration depth, MAP generated by FV and notched needles exceeded the critical threshold for irrigant apical extrusion. MAP generated by SV needle positioned at both 3 mm and 1 mm from the apex was 399.47 and 438Pa, respectively. The negative MAP was generated by MiC [Figure 2b].

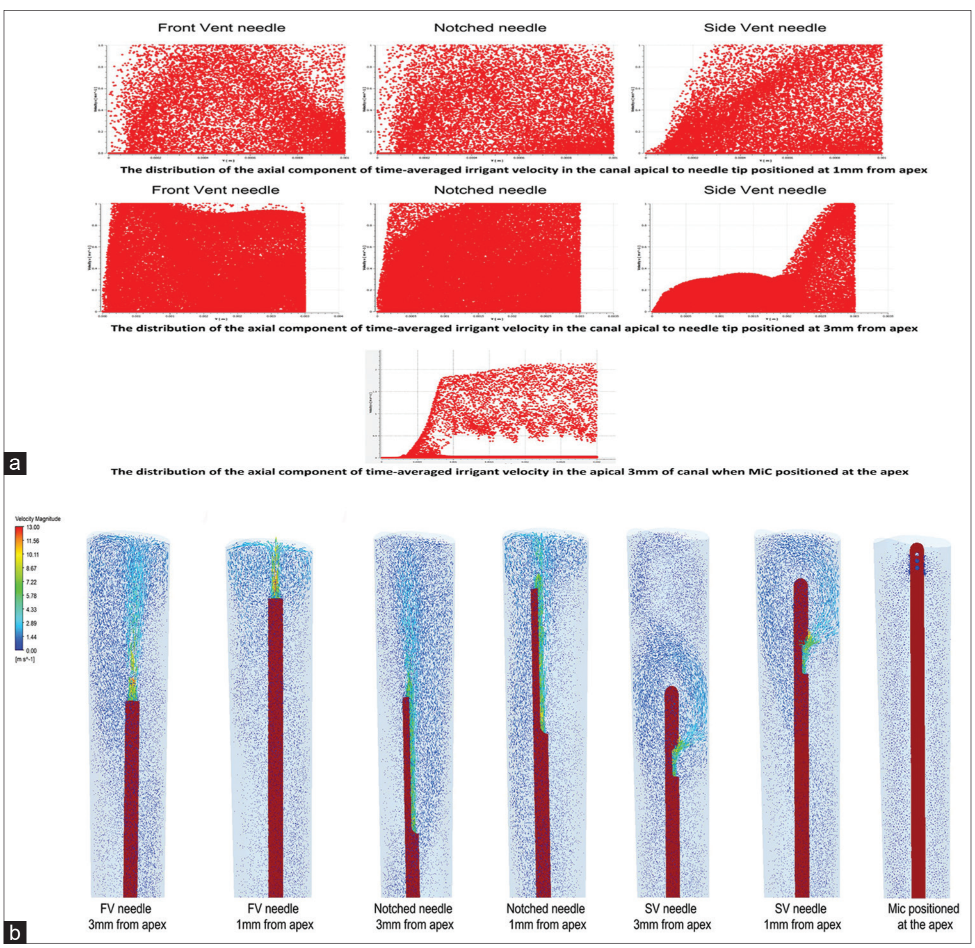

Figure 1: (a) Flow pattern of positive and negative pressure needles, (b) Irrigant velocity in the apical root canal by positive and negative pressure needles. FV: Front vent, SV: Side vent, MiC: Microcannula

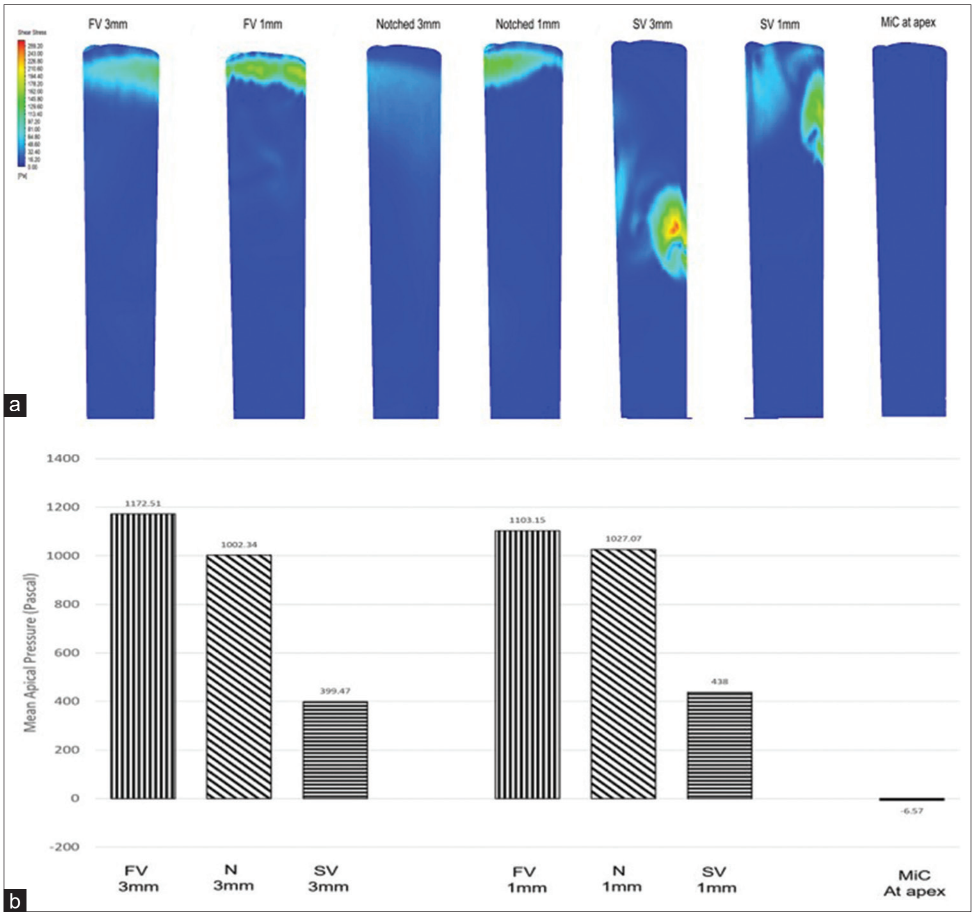

Figure 2: (a) Wall share stress generated by positive and negative pressure needles, (b) Mean apical pressure generated by positive and negative pressure needles. FV: Front vent, SV: Side vent, MiC: Microcannula, N: Notched

Clean depth and clean span

The maximum clean depth was achieved by SV needle placed at 1 mm and the maximum clean span by the notched needle placed at 1 mm [Table 2].

Table 2: Effect of needle working depth on irrigation efficiency

Needle working length	Depth of effective velocity (mm)	Effective shear stress (mm)	
		Clean span	Clean depth
Front vent 3 mm	10.5	9	0.9
Front vent 1 mm	10.5	10	0.1
Notched 3 mm	10.5	0	0
Notched 1 mm	10.5	10.1	0.9
Side vent 3 mm	10.5	7.9	1.4
Side vent 1 mm	10.5	5.6	1.5
MiC at apex	10.5	0	0

MiC: Microcannula

DISCUSSION

The flow parameters of endodontic irrigation in immature teeth are being examined for the first time in this study applying CFD. The CBCT scan was utilized for the 3D reconstruction of root canal geometry. These models generate realistic CFD results as they replicate the internal anatomy and the roughness of the canal wall.[13,14]

To facilitate irrigant penetration and exchange in the apical third and reduce the risk of periapical extrusion, the use of negative pressure irrigation has been advocated in immature teeth. However, A web-based survey of endodontist revealed that only 10% uses a negative pressure irrigation delivery system during endodontic irrigation.[15] Therefore, the present CFD investigation used both positive pressure and negative pressure delivery systems for irrigation simulations.

To reduce the cytotoxicity to stem cells, the American Association of Endodontists[16] advocated the use of 1.5%–3% NaOCl in teeth with necrotic pulp and immature apices. Consequently, the irrigant used in this study was modeled as 2.5% NaOCl. Reynolds stresses were modeled in the present investigation using the SST-k omega turbulent model because it is the only model capable of distinguishing transitional and turbulent flows within the 3D root canal flow domain while preserving fully laminar flow within the needle flow domain.[17]

The CFD simulations in close apex models demonstrated that irrigant extends more than 2 mm beyond the tip in open-ended needles while it is restricted only 1–1.5 mm beyond the needle tip of close-ended needles during positive pressure endodontic irrigation.[11] For appropriate irrigant replenishment, velocities above 0.1 m/s are regarded as clinically significant. The threshold for the removal of biofilm is claimed to be a velocity magnitude of 0.004 m/s.[18] In the present study, the irrigant reached the apex irrespective of the tip design and insertion depth of the needle in all simulations. This observation is in contrast with the study by Boutsioukis *et al.* where the side-vented needle achieved irrigant replacement to the working length only at the 1-mm position.[19] The velocity achieved by FV, SV, and notched needle at 1 mm or 3 mm from the apex was well above the critical threshold of irrigant replacement and biofilm removal.

The drag force required to remove biofilms and debris from canal walls is caused by shear stress, making it a crucial factor to be considered. In accordance with the studies evaluating the impact of the irrigant flow on the depth of the needle insertion, the maximum shear stress generated by open-ended needles in the present study also decreased as the needles moved away from the working length,[19] and the SV needle generated higher WSS on the canal wall facing the outlet. When WSS generated by all the positive pressure needles was compared, FV and SV needles generated maximum WSS when positioned at 1 mm and 3 mm from the apex, respectively, which is in contrast to the findings of a previous study.[10] This difference could be attributed to the divergent walls in the present study instead of tapered canals. According to the mass conservation equation, as the cross-sectional area of the root canal gets larger the velocity of the irrigant decreases, thus reducing the WSS. WSS generated by MiC was negligible with values of 0.7Pa in the apical third of the root canal.

Endodontic irrigation involves the risk of periapical extrusion of irrigant if the pressure exceeds the apical pressure threshold.[20] The apical pressure threshold that needs to be surpassed for extrusion of irrigant is referred to as 25 mmHg (3333 Pa) the capillary pressure,[10] 20–30 mmHg (2666–3999 Pa) the interstitial pressure, and 5.73 mmHg (762 Pa) mean central venous pressure.[21] To err on the side of caution, the mean central venous pressure of 762 Pa was defined as the threshold, and apical pressure values above this threshold were regarded as suggestive of possible apical extrusion. The results of the present study agree with the previous studies, where the open-ended needles at 1 mm generated maximum apical pressure, and the SV needle generated the least apical pressure. All the positive pressure needles used in the study, except SV needle, exceeded the critical threshold of 762 Pa. During negative pressure irrigation, MiC placed at 1 mm from the root end achieved negative values of the MAP in the apical foramen. Hence a negligible risk of irrigant extrusion is expected in both positive-pressure SV needle and negative-pressure MiC irrigation.

The use of the CBCT dataset of a patient to obtain the 3D canal geometry and the use of a prevalidated CFD model were the strengths of the study. Future studies can investigate the effect of different needle designs, i.e., double- or multi-vented, and ultrasonic irrigant activation simulation on WSS and apical pressure during endodontic irrigation of immature teeth.

CONCLUSIONS

The irrigation dynamics in an immature tooth are different from the constantly tapered root canal in a mature tooth. The WSS generated by negative pressure irrigation is insufficient for efficient debridement of the root canal in an immature tooth. The positive pressure irrigation with SV needle positioned within 1 mm of the root apex in immature teeth minimizes the risk of extrusion and generates sufficient WSS to dislodge biofilm in the apical area. The SV needle at 1 mm achieved the maximum clean depth and the notched needle at 1 mm achieved the maximum clean span.

Acknowledgments

All authors affirm that they have no financial affiliation or involvement with any commercial organization with a direct financial interest in the subject or materials discussed in this manuscript, nor have any such arrangements existed in the past 3 years. The authors deny any conflicts of interest related to this study.

Financial support and sponsorship

Nil.

Conflicts of interest

There are no conflicts of interest.

REFERENCES

1. Haapasalo M, Shen Y, Qian W, Gao Y. Irrigation in endodontics. Dent Clin North Am 2010;54:291-312.
2. Galler KM. Clinical procedures for revitalization: Current knowledge and considerations. Int Endod J 2016;49:926-36.
3. Raj S, Dhingra A, Jha P, Nikhil V, Ravinder R, Mishra P. To compare the continuous and intermittent irrigation method on the removal of dentin debris from root canals and to evaluate the dynamics of irrigant flow using computational fluid dynamics. J Conserv Dent 2021;24:94-9.
4. Gopikrishna V, Sibi S, Archana D, Pradeep Kumar AR, Narayanan L. An *in vivo* assessment of the influence of needle gauges on endodontic irrigation flow rate. J Conserv Dent 2016;19:189-93.
5. Sujith IL, Teja KV, Ramesh S. Assessment of irrigant flow and apical pressure in simulated canals of single-rooted teeth with different root canal tapers and apical preparation sizes: An *ex vivo* study. J Conserv Dent 2021;24:314-22.
6. Magni E, Jäggi M, Eggmann F, Weiger R, Connert T. Apical pressures generated by several canal irrigation methods: A laboratory study in a maxillary central incisor with an open apex. Int Endod J 2021;54:1937-47.
7. Dos Reis S, Cruz VM, Hungaro Duarte MA, da Silveira Bueno CE, Vivan RR, Pelegrine RA, *et al.* Volumetric analysis of irrigant extrusion

in immature teeth after different final agitation techniques. J Endod 2020;46:682-7.
8. Velmurugan N, Sooriaprakas C, Jain P. Apical extrusion of irrigants in immature permanent teeth by using endovac and needle irrigation: An *in vitro* study. J Dent (Tehran) 2014;11:433-9.
9. Zhou N, Huang Z, Yu M, Deng S, Fu B, Jin H. Influence of needle working length and root canal curvature on irrigation: A computational fluid dynamics analysis based on a real tooth. BMC Oral Health 2022;22:179.
10. Loroño G, Zaldivar JR, Arias A, Cisneros R, Dorado S, Jimenez-Octavio JR. Positive and negative pressure irrigation in oval root canals with apical ramifications: A computational fluid dynamics evaluation in micro-CT scanned real teeth. Int Endod J 2020;53:671-9.
11. Boutsioukis C, Verhaagen B, Versluis M, Kastrinakis E, Wesselink PR, van der Sluis LW. Evaluation of irrigant flow in the root canal using different needle types by an unsteady computational fluid dynamics model. J Endod 2010;36:875-9.
12. Boutsioukis C, Gutierrez Nova P. Syringe irrigation in minimally shaped root canals using 3 endodontic needles: A computational fluid dynamics study. J Endod 2021;47:1487-95.
13. Leoni GB, Versiani MA, Pécora JD, Damião de Sousa-Neto M. Micro-computed tomographic analysis of the root canal morphology of mandibular incisors. J Endod 2014;40:710-6.
14. Silva EJ, Carvalho CR, Belladonna FG, Prado MC, Lopes RT, De-Deus G, *et al.* Micro-CT evaluation of different final irrigation protocols on the removal of hard-tissue debris from isthmus-containing mesial root of mandibular molars. Clin Oral Investig 2019;23:681-7.
15. Dutner J, Mines P, Anderson A. Irrigation trends among American Association of Endodontists members: A web-based survey. J Endod 2012;38:37-40.
16. American Association of Endodontists. AAE Clinical Consideration for a Regenerative Procedure. Revised 6-8-16. 2016.
17. Gao Y, Haapasalo M, Shen Y, Wu H, Li B, Ruse ND, *et al.* Development and validation of a three-dimensional computational fluid dynamics model of root canal irrigation. J Endod 2009;35:1282-7.
18. Pereira TC, Boutsioukis C, Dijkstra RJ, Petridis X, Versluis M, de Andrade FB, *et al.* Biofilm removal from a simulated isthmus and lateral canal during syringe irrigation at various flow rates: A combined experimental and computational fluid dynamics approach. Int Endod J 2021;54:427-38.
19. Boutsioukis C, Lambrianidis T, Verhaagen B, Versluis M, Kastrinakis E, Wesselink PR, *et al.* The effect of needle-insertion depth on the irrigant flow in the root canal: Evaluation using an unsteady computational fluid dynamics model. J Endod 2010;36:1664-8.
20. Aksel H, Askerbeyli S, Canbazoglu C, Serper A. Effect of needle insertion depth and apical diameter on irrigant extrusion in simulated immature permanent teeth. Braz Oral Res 2014;28:1-6.
21. Charara K, Friedman S, Sherman A, Kishen A, Malkhassian G, Khakpour M, *et al.* Assessment of apical extrusion during root canal irrigation with the novel gentlewave system in a simulated apical environment. J Endod 2016;42:135-9.